



# Catalytic reduction of nitrite in water over ceria- and ceria–zirconia-supported Pd catalysts



Jiyeon Lee<sup>a</sup>, Young Gul Hur<sup>a</sup>, Min-Sung Kim<sup>a,\*</sup>, Kwan-Young Lee<sup>a,b,\*\*</sup>

<sup>a</sup> Department of Chemical and Biological Engineering, Korea University, 145, Anam-ro, Seongbuk-gu, Seoul 136-701, Republic of Korea

<sup>b</sup> Green School, Korea University, 145, Anam-ro, Seongbuk-gu, Seoul 136-701, Republic of Korea

## ARTICLE INFO

### Article history:

Received 8 December 2014

Received in revised form 13 January 2015

Accepted 13 January 2015

Available online 14 January 2015

### Keywords:

Nitrite reduction

Hydrogenation

Ce<sub>1-x</sub>Zr<sub>x</sub>O<sub>2</sub>

Oxygen vacancy

## ABSTRACT

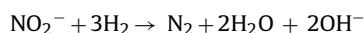
In this study, we tested Pd/Ce<sub>1-x</sub>Zr<sub>x</sub>O<sub>2</sub> catalysts ( $x = 0, 0.3, 0.5$  and  $0.7$ ) for nitrite reduction in water. The Ce<sub>1-x</sub>Zr<sub>x</sub>O<sub>2</sub> was synthesized by the co-precipitation method, and Pd was impregnated on the support using the deposition–precipitation method. The introduction of Zr into the ceria lattice of the catalyst with  $x = 0.3$  and  $0.5$  distorted the lattice structure, accordingly, both the catalysts easily reduced nitrite than the pure CeO<sub>2</sub> supported Pd catalyst. In contrast, the Pd/Ce<sub>0.3</sub>Zr<sub>0.7</sub>O<sub>2</sub> ( $x = 0.7$ ) catalyst became difficult to reduce as the tetragonal ZrO<sub>2</sub> phase was dominant in the catalyst structure. These phenomena led to the difference in the amount of oxygen vacancies on the surface of the catalyst. In the nitrite reduction test, the catalyst containing more oxygen vacancies showed higher activity. The relationships between the catalytic activities and the surface properties with composition of the support over Pd/Ce<sub>1-x</sub>Zr<sub>x</sub>O<sub>2</sub> catalysts were investigated by X-ray diffraction (XRD), Raman spectroscopy and X-ray photoelectron spectroscopy (XPS) analyses.

© 2015 Elsevier B.V. All rights reserved.

## 1. Introduction

In recent years, drinking water is increasingly contaminated with nitrite (NO<sub>2</sub><sup>-</sup>), resulting from the overuse of fertilizer in agriculture and the discharge of industrial wastewater [1]. Because nitrite overexposure in the human body can cause cancer, lung disease and blue-baby syndrome [1–3], the World Health Organization and European Community have determined 0.1 and 0.02 mg/L as the permissible nitrite levels, respectively [2,4]. Because of increasing concerns on the nitrite pollution, various physicochemical (e.g., ion exchange and reverse osmosis) and biological treatments have been used for the nitrite reduction [5,6]; however, each process revealed disadvantage such as need of the secondary treatment process in the former and slow reaction rate in the latter [6]. To solve these problems, Vorlop and Tacke first reported a catalytic reduction method [7] which is performed under mild conditions ( $T = 25^\circ\text{C}$  and  $P = 1$  atm) using a single noble metal supported cata-

lyst and hydrogen gas as the reducing agent, and the reaction is as follows [8]:



Hörold et al. tested diverse noble metal impregnated catalysts, which were Pd, Pt, Ru, Ir and Rh on Al<sub>2</sub>O<sub>3</sub> support, and found that only the Pd supported catalyst was effective for the nitrite reduction [2,8]. Along with active metals, many studies aimed to investigate suitable supports such as Al<sub>2</sub>O<sub>3</sub> [9,10], carbon fiber [11] and conducting polymers [12], because different surface state of the utilized supports could enhance the nitrite reduction. Recently, we studied the performances of Pd–Cu/TiO<sub>2</sub> and Pd–Cu/TiO<sub>2</sub>–CeO<sub>2</sub> catalysts for the nitrate (NO<sub>3</sub><sup>-</sup>) reduction in water [13,14], indicating that oxygen vacancies formed on the reducible TiO<sub>2</sub> and TiO<sub>2</sub>–CeO<sub>2</sub> supports play an important role in promoting the activity. Gavagnin et al. and Guo et al. also claimed that the catalysts including high oxygen vacancy were very active for the nitrate reduction [15,16]. Hence, the study on the effect of oxygen vacancies on the nitrite reduction activity is needed.

The above mentioned studies show that the oxygen vacancies could be generated on reducible oxides (e.g., TiO<sub>2</sub>, CeO<sub>2</sub>, and SnO<sub>2</sub>) [14,15,17]. Furthermore, the formation of oxygen vacancies was also observed on mixed oxides (e.g., Ce<sub>1-x</sub>M<sub>x</sub>O<sub>2</sub>;  $M = \text{Si}^{4+}, \text{Ti}^{4+}$  and  $\text{Zr}^{4+}$ ), resulting from the incorporation of other components into CeO<sub>2</sub> crystalline lattice, thereby changing the textural properties

\* Corresponding author. Tel.: +82 2 3290 3299; fax: +82 2 926 6102.

\*\* Corresponding author. Tel.: +82 2 3290 3727; fax: +82 2 926 6102.

E-mail addresses: [calmlive@korea.ac.kr](mailto:calmlive@korea.ac.kr) (M.-S. Kim), [kylee@korea.ac.kr](mailto:kylee@korea.ac.kr) (K.-Y. Lee).

[18–20]. Among different materials, the  $\text{Ce}_{1-x}\text{Zr}_x\text{O}_2$  mixed oxides have been widely used in various research areas. For Pt catalysts in the partial oxidation of methane, the addition of Zr to the  $\text{CeO}_2$  lattice increased the number of oxygen vacancies, enhancing the performance of  $\text{Pt/Ce}_{1-x}\text{Zr}_x\text{O}_2$  than that of  $\text{Pt/CeO}_2$  [21]. Similarly, the oxygen vacancies on the  $\text{Ce}_{1-x}\text{Zr}_x\text{O}_2$  supported Cu catalysts acted as active sites for capturing CO and  $\text{CO}_2$ , and consequently, high yield of methanol from  $\text{CO/CO}_2/\text{H}_2$  gas was obtained using  $\text{Cu/Ce}_{0.7}\text{Zr}_{0.3}\text{O}_2$  catalyst [22]. Based on these studies, we proposed  $\text{Ce}_{1-x}\text{Zr}_x\text{O}_2$  as promising support materials for the nitrite reduction. Thus, our objective was to investigate the effect of the oxygen vacancy on the catalytic nitrite reduction in water over a series of  $\text{Pd/Ce}_{1-x}\text{Zr}_x\text{O}_2$  catalysts with varying Zr contents.

## 2. Experimental

### 2.1. Catalyst preparation

$\text{Ce}_{1-x}\text{Zr}_x\text{O}_2$  ( $x=0, 0.3, 0.5, 0.7$ ) supports were prepared by the co-precipitation method described in the previous studies [22–24]. Stoichiometric amount of cerium(III) nitrate hexahydrate ( $\text{Ce}(\text{NO}_3)_3 \cdot 6\text{H}_2\text{O}$ , Aldrich, 99%) and zirconium(IV) oxide chloride octahydrate ( $\text{ZrOCl}_2 \cdot 8\text{H}_2\text{O}$ , Sigma–Aldrich, 98%) were dissolved in deionized water (solution; 0.1 M), which was adjusted pH to 8 using ammonium hydroxide (28%  $\text{NH}_4\text{OH}$ , Sigma–Aldrich). The solution was vigorously stirred at 80 °C for 3 h and then washed using deionized water until chloride ion was not detected. The washed sample was dried at 100 °C for 24 h, followed by calcined at 400 °C for 4 h in air.

Pd was impregnated using the deposition–precipitation method [25], and the amount of Pd was fixed at 3 wt.% in all the catalysts. Palladium chloride ( $\text{PdCl}_2$ , Aldrich, 99.9%) and the synthesized support were dissolved in 0.01 M of HCl solution, which was then heated to 75 °C. Thereafter, 1 M  $\text{Na}_2\text{CO}_3$  solution was slowly added to the mixed solution under vigorous stirring until a pH of 10 was reached. After 3 h of stirring, the solution was filtered and washed several times with deionized water. The resulting solid was dried at 100 °C overnight and calcined at 400 °C for 4 h. Finally, all the prepared catalysts were reduced with  $\text{H}_2/\text{N}_2$  (10% vol%) at 200 °C for 2 h before the reaction tests. The abbreviations of the  $\text{Pd/Ce}_{1-x}\text{Zr}_x\text{O}_2$  catalysts are listed in Table 1.

### 2.2. Catalyst characterization

The contents of Pd and Ce/Zr molar ratio in the  $\text{Pd/Ce}_{1-x}\text{Zr}_x\text{O}_2$  catalysts were analyzed by inductively coupled plasma atomic emission spectroscopy (ICP–AES, Thermo Instrument, Polyscan 61E). The surface areas of catalysts were measured by the nitrogen adsorption–desorption method using a BET instrument (BEL Japan Inc. BELSORP MAX). Before the measurement, catalysts were pretreated at 373 K under vacuum to remove the moisture and impurities in the catalysts.

X-ray diffraction (XRD) was performed using an X-ray powder diffractometer (Rigaku, ATX-G) using Cu K $\alpha$  ( $\lambda = 1.5406 \text{ \AA}$ )

irradiation to determine the crystal structure of the support and palladium. The diffraction patterns were scanned in the  $2\theta$  range from 10° to 80° at a scanning rate of 2°/min. Raman spectra were recorded at room temperature using a Raman spectrometer (Horiba Jobin Yvon, LabRam Aramis). The data were detected with 514.5 nm line of Ar-ion laser. X-ray photoelectron spectroscopy (XPS) was performed with a PHI 5000 Versa Probe equipped with an Al K $\alpha$  X-ray source (1486.6 eV), and binding energies were corrected with C1s referenced at 284.6 eV.

### 2.3. Reaction test

The reaction test was performed on a semi batch reactor at 25 °C and atmospheric pressure. Before the test, the catalyst (0.3 g) was suspended in 295 mL of deionized water and purged with nitrogen to remove remaining air. After the purging, hydrogen gas at a flow rate of 90 mL/min was used as the reducing agent, and 5 mL of nitrite solution (2 mM of  $\text{KNO}_2$ , Sigma–Aldrich) was injected in the reactor. In order to improve the activity,  $\text{CO}_2$  gas was added as a pH buffer.

During the reaction test, the samples were periodically withdrawn to estimate the catalytic performance. Nitrite ion concentration was determined by high performance liquid chromatography (Young-Lin) using a Zorbax Eclipse C18 column with a UV detector at a wavelength of 210 nm. The mobile phase consisted of 0.01 M of octylammonium orthophosphate and methanol. Ammonium ion was measured using ion chromatography (Dionex, thermal conductivity detector) with an IonPac CS12A column and methanesulfonic acid (20 mM) as the mobile phase.

The conversion of nitrite was calculated by Eq. (1).

$$\text{Nitrite Conversion, } X_{\text{NO}_2^-}(\%) = \frac{C(\text{NO}_2^-)_i - C(\text{NO}_2^-)_f}{C(\text{NO}_2^-)_i} \times 100 \quad (1)$$

The selectivity of ammonium ion and nitrogen yield were calculated by Eqs. (2) and (3).

$$\text{Ammonium selectivity, } S_{\text{NH}_4^+}(\%) = \frac{C(\text{NH}_4^+)}{C(\text{NO}_2^-)_i - C(\text{NO}_2^-)_f} \times 100 \quad (2)$$

$$\text{Nitrogen yield } (\%) = \frac{X_{\text{NO}_2^-} \times (100 - S_{\text{NH}_4^+})}{100} \quad (3)$$

## 3. Results and discussion

### 3.1. BET, XRD and Raman analysis

BET surface areas and pore volumes of  $\text{Pd/Ce}_{1-x}\text{Zr}_x\text{O}_2$  catalysts (PC and PCZ) are listed in Table 1. The specific surface area increased with increasing Zr content (i.e.,  $\text{PC} \rightarrow \text{PCZ}$ ), and the present result was similar to those reported by Levasseur et al. and Terribile et al. [26,27]. The trend of surface area variation might arise from that the Zr insertion-induced phase transformation from a cubic  $\text{CeO}_2$  to a tetragonal  $\text{ZrO}_2$ , preventing the sintering of the catalysts, and the results were consistent with the XRD result. In contrast, there was no relationship between the Zr content and pore volume.

**Table 1**  
Chemical compositions and BET properties of the  $\text{Pd/Ce}_{1-x}\text{Zr}_x\text{O}_2$  catalysts.

Material	Composition <sup>a</sup>		CeO <sub>2</sub> /ZrO <sub>2</sub> (molar ratio)	Surface area (m <sup>2</sup> /g)	Pore volume (cm <sup>3</sup> /g)
	Abbreviation	Pd (wt.%)			
$\text{Pd/CeO}_2$	PC	3.0	100.0/0	7.5	0.043
$\text{Pd/Ce}_{0.7}\text{Zr}_{0.3}\text{O}_2$	PCZ1	2.9	69.4/30.6	68.9	0.148
$\text{Pd/Ce}_{0.5}\text{Zr}_{0.5}\text{O}_2$	PCZ2	2.9	49.4/50.6	82.7	0.097
$\text{Pd/Ce}_{0.3}\text{Zr}_{0.7}\text{O}_2$	PCZ3	3.0	29.9/70.1	92.0	0.072

<sup>a</sup> Determined by ICP–AES.

Download English Version:

<https://daneshyari.com/en/article/65181>

Download Persian Version:

<https://daneshyari.com/article/65181>

[Daneshyari.com](https://daneshyari.com)